1

INSIGHTS INTO THE PROPOSED COPPER–OXYGEN INTERMEDIATES THAT REGULATE THE MECHANISM OF REACTIONS CATALYZED BY DOPAMINE β-MONOOXYGENASE, PEPTIDYLGLYCINE α-HYDROXYLATING MONOOXYGENASE, AND TYRAMINE β-MONOOXYGENASE

ROBERT L. OSBORNE

Department of Chemistry and California Institute for Quantitative Biosciences, University of California, Berkeley, CA 94720

JUDITH P. KLINMAN

Department of Chemistry, Department of Molecular and Cellular Biology, and California Institute for Quantitative Biosciences, University of California, Berkeley, CA 94720

Copper-Oxygen Chemistry, First Edition. Edited by Kenneth D. Karlin and Shinobu Itoh.

1.1. GENERAL INTRODUCTION

Oxidation–reduction reactions are essential to all biological systems and are involved in energy storage and countless biosynthetic reactions. Monooxygenases represent a large class of redox enzymes that incorporate one atom from dioxygen (O_2) into organic substrates while the other oxygen appears in water (Eq. 1.1).[1]

$$R_3C{-}H + O_2 + 2H^+ + 2e^- \rightarrow R_3C{-}OH + H_2O \qquad (1.1)$$

Without monooxygenases, the spin-forbidden hydroxylation of innumerable ground-state singlet organic substrates by ground-state triplet O_2 would not occur at measurable rates. Nature has evolved to utilize organic cofactors and transition metal ions in order to bypass the spin-forbidden properties of these reactions. The total number of copper-containing monooxygenases is relatively small, but they catalyze physiologically essential reactions and are of great interest to medical science.[2] This chapter focuses on the chemical mechanism of dopamine β-monooxygenase (DβM), peptidylglycine α-hydroxylating monooxygenase (PHM), and tyramine β-monooxygenase (TβM), which belong to a small class of homologous, eukaryotic copper-, ascorbate-, and oxygen-dependent enzymes.[3–5] Herein, we aim to highlight parallel features that are unique to the members of this important class of enzymes. In particular, spectroscopic, structural, and detailed kinetic analyses are critically examined, discussed, and compared to the significant, recent contributions to the literature. A re-examination of previous findings, together with recent evidence, points toward a network of communication between the two copper-containing domains that are separated by an 11Å, solvent-filled cleft. The goal of this chapter is to provide a comprehensive examination of the complex mechanism of O_2 activation coupled to hydrogen atom transfer catalyzed by this fascinating class of enzymes.

1.2. COMPARATIVE PROPERTIES OF DOPAMINE β-MONOOXYGENASE (DβM), PEPTIDYLGLYCINE α-HYDROXYLATING MONOOXYGENASE (PHM), AND TYRAMINE β-MONOOXYGENASE (TβM)

Dopamine β-monooxygenase (DβM) is an essential enzyme in the catecholamine biosynthetic pathway that catalyzes the hydroxylation of dopamine to yield norepinephrine (Eq. 1.2), both of which are neurotransmitters in the sympathetic nervous system.[6–8]

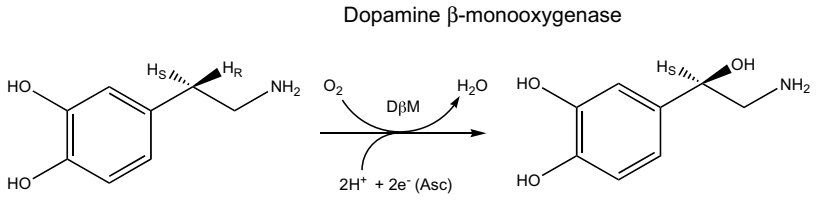

(1.2)

Dopamine

Norepinephrine

Asc = ascorbate

Peptidylglycine α-amidating monooxygenase (PAM) is a bifunctional enzyme, which contains two independent enzymatic domains: a monooxygenase domain and a lyase domain. Peptidylglycine α-hydroxylating monooxygenase (PHM) is the monooxygenase domain and catalyzes the hydroxylation of peptidylglycine substrates (Eq. 1.3) en route to the biosynthesis of C-terminally carboxamidated peptide hormones.[4,9]

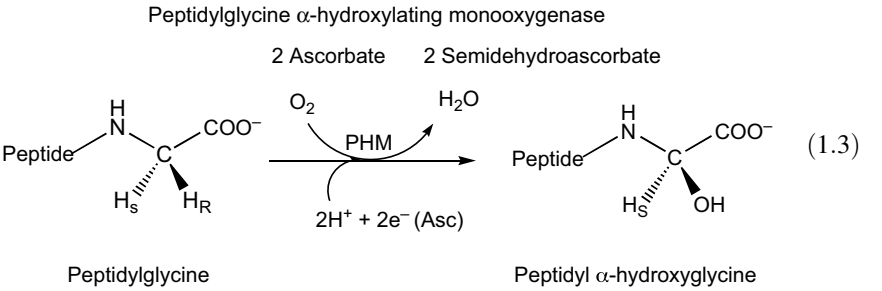

(1.3)

Tyramine β-monooxygenase (TβM) is the insect homologue of DβM and plays a critical role in the biosynthesis of invertebrate neurotransmitters by catalyzing the hydroxylation of tyramine (Eq. 1.4).[10–12]

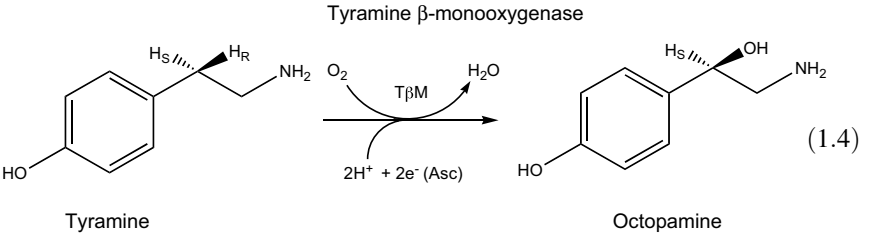

(1.4)

The enzymes DβM and PHM exist in both soluble and membrane-bound forms localized in neurosecretory vesicles of the adrenal gland or synaptic vesicles of the sympathetic nervous system (DβM) or secretory vesicles of the pituitary gland (PHM).[9,13–15] The location of TβM expression is not definitively known, but studies indicate that TβM is localized to octopaminergic neurons.[11,12] Initial studies on this important class of enzymes were focused on DβM. However, extensive experimental evidence, which will be discussed throughout this chapter, indicates a highly conserved chemical mechanism among all three enzymes.

The two-electron ($2e^-$) oxidation of dopamine to norepinephrine (Eq. 1.2), C-terminal glycine-extended peptides to their α-hydroxylated products (Eq. 1.3), and tyramine to octopamine (Eq. 1.4) involves the incorporation of an oxygen atom into the β-carbon of the ethylamine side chain (DβM and TβM) or the α-carbon of peptide hormone precursors (PHM). Early experiments revealed that DβM was a copper-dependent enzyme and that the incorporated oxygen was derived from molecular oxygen. However, understanding the relationship between copper

stoichiometry and enzyme activity remained a challenge until rapid mixing techniques were used to demonstrate that optimal catalysis required two copper atoms per DβM subunit.[16] Electron paramagnetic resonance (EPR) spectra collected for PHM samples reconstituted with copper were found to contain ~ 2 equiv of copper per mole of enzyme.[4] Substrate oxidation is coupled to the $4e^-$ reduction of O_2 to water by using two electrons stored on copper cofactors of the enzyme, supplied by an exogenous donor, and two from the substrate undergoing oxidation. The preferred *in vitro* and *in vivo* electron donor is ascorbic acid, which is oxidized sequentially to yield 2 equiv of semidehydroascorbate with concomitant cyclical reduction of the copper sites.[17–21] The Cu(I) sites are recycled to Cu(II) in the presence of substrate and O_2 via a "ping–pong" mechanism.

Despite numerous efforts, a robust DβM expression system has not been developed. However, the availability of a fully active truncated PHM expression system[4] and the very recently developed facile TβM expression system[21] has made the pursuit of structure–function–dynamics relationships possible.

1.3. SEQUENCE, STRUCTURE, AND SPECTROSCOPY

Comparison of the primary sequence of PHM with a core of ~300 amino acids from DβM indicates 27% identity and 40% similarity.[4,22,23] The sequence of TβM is 39% identical and 55% similar to its mammalian equivalent, DβM (Fig. 1.1).[21,24] Among these enzymes are six conserved copper ligands. Eight of the 10 cysteine residues in PHM are conserved.[4,15] The 12 intrasubunit cysteine residues of DβM are conserved in TβM, but the intersubunit cysteines of DβM are not conserved.[21] However, only five cysteine residues are strictly conserved when the primary sequences of DβM (rat), PHM (rat), and TβM (*Drosophila*) are aligned (Fig. 1.1).[24] In the last decade, a series of X-ray crystal structures of different forms of the catalytic core of PHM have been published that are fully consistent with previous indirect structural probes and spectroscopic studies. PHM is composed of two domains ~150 residues in length, each of which contains one catalytic copper (Fig. 1.2).[25] The domain structures include an eight-stranded antiparallel jelly-roll motif. The solvent-exposed active-site coppers are separated by ~11 Å, and the coordination environment of each copper is unique (Fig. 1.3).[25] The unusually long distance between copper sites without bridging ligands is consistent with earlier EPR studies in which no evidence of spin coupling between the paramagnetic copper centers was detected.[2] The EPR studies on PHM and TβM further support the structural homology between the copper centers among this class of enzymes.[4,21]

Extended X-ray absorption fine structure (EXAFS) spectroscopy has been used to probe the coordination environment of DβM and PHM and, most recently, TβM. The EXAFS data for oxidized Cu(II) proteins reveal an average of 2.5 N (histidine) and 1.5 O or N ligands per copper at 1.97 Å.[4,26–29] In addition, a weak sulfur ligand is detected at 2.71 Å in PHM[4] in agreement with the Cu_M site visualized in the crystal structure.[25] The EXAFS studies of reduced Cu(I) proteins detect a shorter sulfur ligand distance (2.27 Å in PHM, 2.25 Å in DβM, and 2.24 Å in TβM) than in the oxidized

```
DBM    ------------------------------------MQPHLSHQPCWSLP 14
TBM    MLKIPLQLSSQDGIWPARFARRLHHHHQLAYHHHKQEQQQQQQQQQQQQA 50
PHM    --------------------------------------------------

DBM    SPSVREAASMYG---TAVAIFLVILVAALQG------SEPPESPFPYHIP 55
TBM    KQKQKQNGVQQGRSPTFMPVMLLLLMATLLTRPLSAFSNRLSDTKLHEIY 100
PHM    --------------------------------------------------

DBM    LDPEGTLELSWNVSYDQEIIHFQLQ--VQGPRAGVLFGMSDRGEMENADL 103
TBM    LD-DKEIKLSWMVDWYKQEVLFHLQNAFNEQHRWFYLGFSKRGGLADADI 149
PHM    --------------------------------------------------

DBM    VMLWTDGDRTYFADAWSDQKGQIHLDTHQDYQLLQAQRVSNSLSLLFKRP 153
TBM    CFFENQNG--FFNAVTDTYTSPDGQWVRRDYQQDCEVFKMDEFTLAFRRK 197
PHM    --------------------------------------------------

DBM    FVTCDPKDYVIEDDTVHLVYG-----ILEEPFQSLEAINTSGLHTGLQQV 198
TBM    FDTCDPLDLRLHEGTMYVVWARGETELALEDHQFALPNVTAPHEAGVKML 247
PHM    ----------------------------------------------N 45

DBM    QLLKPEVSTPAMPADVQTMDIRAPDVLIPSTETTYWCYITELPLHFPR-H 247
TBM    QLLRADK-ILIPETELDHMEITLQEAPIPSQETTYWCHVQRLEGNLRRRH 296
PHM    ECLGTIGPVTPLDASDFALDIRMPG-VTPKESDTYFCMSMRLP--VDEEA 92
         *                  *       *    ** *    *

DBM    HIIMYEAIVTEGNEALVHHMEVFQCTN-ESEAFPMFNGPCDSKMKPDRLN 296
TBM    HIVQFEPLIR--TPGIVHHMEVFHCEAGEHEEIPLYNG--DCEQLPPRAK 342
PHM    FVIDFKPRAS---MDTVHHMLLFGCNMPSSTGSYWFCDEGTCTDKAN--- 136
                     ****  * *

DBM    YCRHVLAAWALGAKAFYYPEEAGVPLGSSGSSRFLRLEVHYHNPRNIQG- 345
TBM    ICSKVMVLWAMGAGTFTYPPEAGLPIGGPGFNPYVRLEVHFNNPEKQSG- 391
PHM    ----ILYAWARNAPPTRLPKGVGFRVGGETGSKYFVLQVHYGDISAFRDN 182
              **  *     *   *   *          * **

DBM    RRDSSGIRLHYTASLRPNEAGIMELGLVYTPLMAIPPQETTFVLTGYCTD 395
TBM    LVDNSGFRIKMSKTLRQYDAAVMELGLEYTDKMAIPPGQTAFPLSGYCVA 441
PHM    HKDCSGVSVHLTRVPQP---LIAGMYLMMSVDTVIPPGEKVVNAD----I 225
         * **                     *       ***

DBM    RCTQMALPKSGIRIFASQLHTHLTGRKVITVLARDGQQREVVNRDNHYSP 445
TBM    DCTRAALPATGIIIFGSQLHTHLRGVRVLTRHFRGEQELREVNRDDYYSN 491
PHM    SCQYKMYP---MHVFAYRVHTHHLGKVVSGYRVRNGQWTLIGRQNPQLP- 271
        *     *      *    ***  *  *     *  *

DBM    HFQEIRMLKNAVTVHQGDVLITSCTYNTENRTMATVGGFGILEEMCVNYV 495
TBM    HFQEMRTLHYKPRVLPGDALVTTCYYNTKDDKTAALGGFSISDEMCVNYI 541
PHM    --QAFYPVEHPVDVTFGDILAARCVFTGEGRTEATHIGGTSSDEMCNLYI 319
         *          *  ** *   *          *   *     ***  *

DBM    HYYPKTELELCKSAVDDGFLQKYFHIVNRFGNEEVCTCPQASVPQQFASV 545
TBM    HYYPATKLEVCKSSVSEETLENYFIYMKRTEHQHGVHLNGARS-SNYRSI 590
PHM    MYYMEAKYALSFMTCTKNVAPDMFRTIPAEANIPI---------------- 354
        **                   *

DBM    PWNSFNRDMLKALYNYAPISVHCNKTSAVRFPGNWNLQPLPKITSAVEEP 595
TBM    EWTQPRIDQLYTMYMQEPLSMQCNRSDGTRFEGRSSWEGVAATPVQIRIP 640
PHM    --------------------------------------------------

DBM    DPRCPIRQTRGPAGPFVVITTEADTE----- 621
TBM    -IHRKLCPNYNPLWLKPLEKGDCDLLGECIY 670
PHM    -------------------------------
```

FIGURE 1.1. Sequence alignment of the mononuclear copper-containing monooxygenases using Clustal W 2.0.10.[24] Sequences for DβM and PHM are from rat and TβM from *Drosophila melanogaster*. Metal-binding ligands are shown in bold and underlined and conserved cysteine residues in italic and underlined. All conserved residues are indicated with a ⋆ below the sequences.

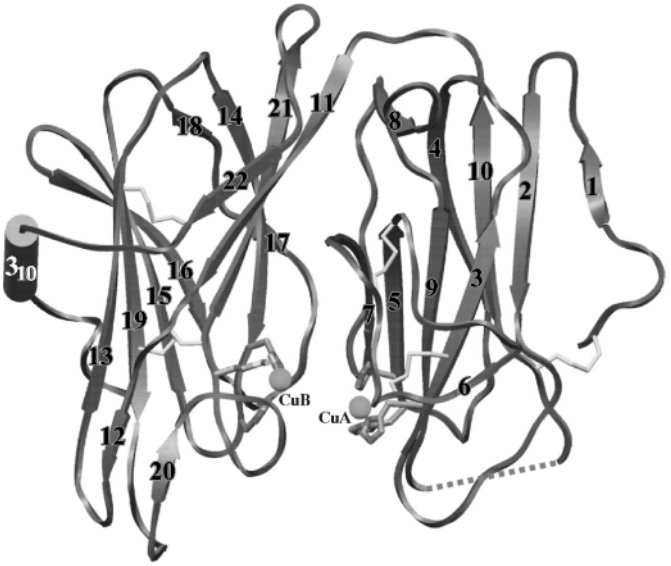

FIGURE 1.2. A representation of the catalytic core of PHM. The backbone is shown in gray with the catalytic coppers represented by green spheres. Strands are numbered arrows and the cylinder is a 3_{10} helix. Side chains of ligands to the two catalytic coppers (green spheres) are colored by atom type (carbon is gray, nitrogen is blue, sulfur is yellow). The dashed gray line indicates a six-residue loop (I176 to D181) not built into the final model. This figure[25] is from Prigge, S. T.; Eipper, B. A.; Mains, R. E.; Amzel, L. M. Amidation of bioactive peptides: The structure of peptidylglycine α-hydroxylating monooxygenase *Science* **1997**, *278,* 1300–1305. (Reprinted with permission from AAAS.) (See color insert.)

enzymes.[4,27–29]X-ray absorption spectroscopy (XAS) experiments indicate that the copper geometry of PHM in solution is predominately four-coordinate with some contribution of five-coordinate geometry.[26] As Figure 1.3 illustrates, these spectroscopic structural probes are in reasonable agreement with the copper sites observed crystallographically. Domain I binds one active site copper, designated Cu_H (Cu_A on the right), by three histidine residues (His107, His108, and His172) (Fig. 1.3). Domain II coordinates the second catalytic copper, Cu_M (Cu_B on the left), with two histidines and a methionine residue (His242, His244, and Met314).[25] Previous studies established that substrate hydroxylation is catalyzed at the Cu_M domain through a radical-initiated hydrogen-atom abstraction mechanism.[30–32] Spectroscopic, kinetic, and structural analyses support a mechanism whereby O_2 and substrate bind to the Cu_M site during catalysis.[27,32–35] The Cu_H site is assigned the role of an electron reservoir that supplies the second electron required for hydroxylation of the C−H bond by long-range intramolecular electron transfer (ET) from Cu_H to Cu_M.[33] An early structure of PHM in the presence of a substrate analogue, *N*-α-acetyl-3,5-diiodotyrosylglycine, bound at the Cu_M site, showed no change in the 11 Å distance between copper sites (i.e., the failure of the two copper sites to move closer together when substrate is present).[25]

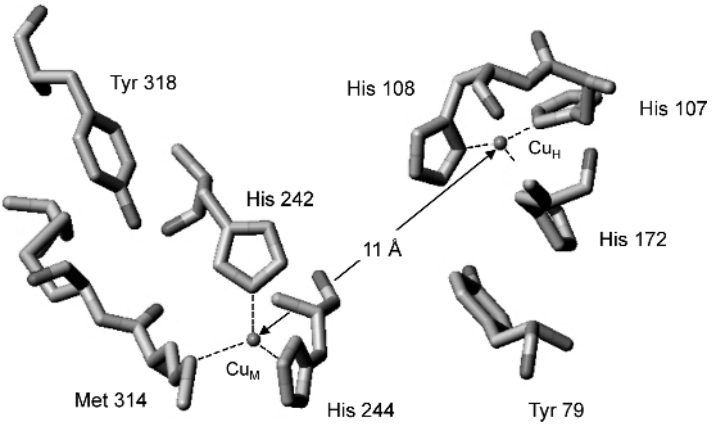

FIGURE 1.3. (Recreated from PDB: 1PHM).[25] The coordination environment of Cu_M (His242, His244, and Met314), Cu_H (His107, His108, and His172), and the relationship of Tyr79 and Tyr318 to the active site coppers of PHM.

1.4. ENZYME MECHANISMS DERIVED FROM KINETIC CHARACTERIZATION AND KINETIC ISOTOPE EFFECTS

One of the primary goals in the mechanistic characterization of the coupling of O_2 to substrate activation for DβM, PHM, and TβM has been to isolate the individual chemical steps of the reaction from substrate binding to product release. Klinman et al.[36] pioneered the use of kinetic isotope effects (KIEs) to delineate complex kinetic mechanisms, showing that the order of addition of reactants can be determined for multireactant enzymes from the magnitude of the isotope effects on the kinetic parameters for the various substrates.[36] Earlier studies with DβM had led to the proposal of an equilibrium-ordered mechanism in which O_2 binds prior to substrate.[37] In accord with this mechanism, the KIE on V_{max}/K_m for substrate would be independent of O_2 concentration. Contrarily, the primary tritium KIE was found to be dependent on O_2 concentration, providing the first unequivocal evidence for a random kinetic mechanism for DβM catalysis (Scheme 1.1).[36] The kinetic mechanism for PHM was subsequently determined using protiated and dideuterated hippuric acid as substrate. The initial rate patterns and double-reciprocal plots are indicative of an equilibrium-ordered mechanism with O_2 binding after hippuric acid to reduced PHM (Scheme 1.2).[38] Similarly, the kinetic characterization of TβM has recently been completed using protiated and dideuterated tyramine. Analogous to DβM, the kinetic data support a random mechanism where either tyramine or O_2 can bind first to reduced TβM (Scheme 1.1). The most notable difference between the kinetic mechanism of DβM and TβM is the substrate inhibition observed for the reaction of TβM with tyramine. The pattern of substrate inhibition indicates tyramine can interact with oxidized TβM to form an inhibitory complex, E·Cu(II)·S. The observed inhibition and kinetic profile of TβM suggest a tighter regulation of neurotransmitter levels in insects.[39]

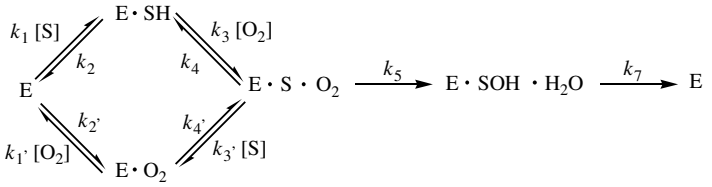

SCHEME 1.1. Kinetic mechanism for random-ordered binding of substrate and O_2.

The reactions catalyzed by this class of enzymes require the abstraction of a hydrogen atom from substrate by the activated oxygen species to yield hydroxylated product and water. Thus, the use of isotopically labeled substrates as mechanistic probes has served as a powerful tool for delineating complex chemical and kinetic mechanisms. The magnitude of primary KIEs for solution reactions can be equal to the intrinsic KIE because the chemical step is rate determining. However, the kinetic complexity of enzyme-catalyzed reactions often results in diminished primary KIEs given that substrate activation is only partially rate limiting. Such is the case when using deuterated dopamine, hippuric acid, and tyramine for reactions catalyzed by DβM, PHM, and TβM, respectively, resulting in comparatively small experimental KIEs under steady-state conditions.[38–40] Accordingly, isolation of the C−H bond cleavage step in enzyme-catalyzed reactions and the measurement of the intrinsic primary KIE is essential for accurate interpretation of steady-state KIEs. The method developed by Northrop[41] made it possible to extract the intrinsic primary KIE, and this method has been applied to DβM and PHM catalyzed reactions (Table 1.1).[38,40,42,43]

The intrinsic primary KIE for the reaction of DβM with dopamine yields a value of 10.9 ± 1.9.[40] Subsequently, this value was used in concert with a structure–reactivity study of a series of para-substituted phenethylamines to calculate the rate constant for the C−H bond cleavage step during DβM-catalyzed reactions.[32] Equation 1.5 demonstrates how the rate of C−H bond cleavage (k_{C-H}) can be calculated using the rate constant for protiated substrate (k_{cat}), the intrinsic KIE for dopamine (^Dk), and the observed KIE on k_{cat} ($^Dk_{cat}$).

$$k_{C-H} = k_{cat}(^Dk - 1)/[^Dk_{cat} - 1] \tag{1.5}$$

The observed increase in rate with ring-donating substituents was initially interpreted to be the result of an electron-deficient transition state resulting from O_2. However,

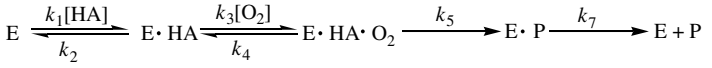

SCHEME 1.2. Kinetic mechanism for equilibrium-ordered binding of substrate before O_2.

TABLE 1.1. Primary and Secondary Intrinsic Hydrogen and Oxygen Isotope Effects Demonstrating the High Conservation of Mechanism between DβM and PHM[a]

Enzyme	Intrinsic		Observed	
	k_H/k_D for C−H		k_{16}/k_{18} for O−O	
	1°	2°	C−H	C−D
DβM	10.9	1.19	1.0197	1.0256
	(1.9)	(0.06)	(0.0003)	(0.0003)
PHM	10.6	1.20	1.0167	1.0216
	(0.8)	(0.03)	(0.0032)	(0.0014)

[a] This table was derived from Refs. 38, 40, 42 and 43.

a modified Marcus model (i.e., for ground-state tunneling) whereby hydrogen transfer occurs quantum mechanically (Eq. 1.6), is now used to express the hydrogen-transfer reaction catalyzed by DβM.[42]

$$k_{tun} = \exp\left\{ -(\Delta G^\circ + \lambda)^2 \Big/ (4\lambda RT) \right\} \int_{r_1}^{r_0} \exp^{-m_H \omega_H r^2{}_H / 2\hbar} \exp^{-E_X/k_B T} dX \qquad (1.6)$$

According to Eq. 1.6, ΔG° is the reaction driving force; λ is the environmental reorganization; m_H, ω_H, and r_H are the mass, frequency and distance traveled for the transferred particle; E_x is the barrier for inter nuclear distance sampling with $\hbar$, k_B, R and T, Planck's constant over 2π, Boltzmann's constant, the gas constant, and temperature, respectively. According to the formalism in Eq. 1.6, the transition state for hydrogen transfer reflects the motions of the heavy atoms of the environment and not the cleavage of the C−H bond *per se*. In this context, the structure–reactivity correlations reported earlier for DβM are reflective of the changing ΔG° among substrates with varying structures. Although the ability to correlate the k_{tun} of Eq. 1.6 with ΔG° would be of considerable interest, there are currently neither computational nor experimental estimates for the size of ΔG° that represents the equilibration between phenethylamine substrates and the substrate-derived free radical.

Evidence for hydrogen transfer by a quantum mechanical mechanism for the PHM-catalyzed reaction has come from the kinetic isolation of the hydrogen-transfer step from other partially rate-limiting steps and determination of the intrinsic KIE as a function of temperature. The intrinsic primary KIE is nearly temperature-independent within experimental error. A fit of the intrinsic KIE to the Arrhenius equation for isotope effects (Eq. 1.7) yields $A_H/A_D = 5.9 \pm 3.2$

$$^{D}k_{int} = A_H/A_D \exp\{[E_a(D) - E_a(H)]/RT\} \qquad (1.7)$$

and $E_a(D) - E_a(H) = 0.37 \pm 0.33$ kcal/mol.[42] These values lie significantly outside semiclassical limits [$0.7 < A_H/A_D < 1.4$ and $E_a(D) - E_a(H) = 1.2$ kcal/mol] and cannot be explained by a tunneling correction model.[44–46] Additionally, the combined magnitudes of the intrinsic primary and secondary KIEs (Table 1.1) cannot be rationalized by classical theory.

The relationship between hydrogen and O_2 activation in this class of enzymes can be further probed by measuring an oxygen KIE. The ability to detect small changes in ^{16}O and ^{18}O by mass spectrometry permits precise quantification of the oxygen KIE that can be related to the structure of the activated oxygen at Cu_M. Further, comparing the magnitude of the oxygen KIE using both protio and deuterio substrates allows discrimination among a range of possible mechanisms. At least six mutually exclusive mechanisms for O_2 activation by DβM, PHM, and TβM have been posited: (A) formation of a $2e^-$ reduced Cu_M(II)-hydroperoxo or (B) Cu_M(II)-peroxo species, (C) reductive cleavage of a Cu_M(II)-hydroperoxo intermediate by a conserved active-site tyrosine to form a Cu_M(II)-oxo species, (D) a superoxide-channeling mechanism, whereby O_2 initially binds at Cu_H to form a Cu_H-superoxide intermediate, which dissociates and migrates across a solvent interface to bind to and be further reduced at the Cu_M site,[47,48] (E) a mechanism where the function of the coppers is reversed with substrate hydroxylation occurring via a Cu_H(II)-superoxide intermediate,[49] and (F) a $1e^-$ reduced Cu_M(II)-superoxo intermediate.

The propensity and favorable energetics for hydrogen peroxide (H_2O_2) formation from O_2 led to an initial focus on mechanisms A and B above. To test for the formation of a Cu_M(II)-hydroperoxo species (mechanism A), it was reasoned that generation of such an intermediate at the highly solvent-exposed active site upon reaction could result in uncoupling between O_2 activation and substrate hydroxylation. However, full coupling of O_2 consumption and product formation was observed in studies with DβM using a range of substrates that varied by three-orders of magnitude in reactivity.[50] Similarly, tight coupling of O_2 uptake and product formation was observed for H172A PHM, a variant at Cu_H that retains its copper-binding and hydroxylase activity yet results in a three-order of magnitude decrease in k_{cat}.[51] Contrarily, formation of metal hydroperoxide intermediates in other enzymes (i.e., cytochrome P450s) often involves concomitant uncoupling of substrate hydroxylation and O_2 reduction.[52,53] Additionally, the experiments described above appear to rule out a superoxide channeling mechanism (mechanism D) based on the high probability of some degree of uncoupling between O_2 and substrate activation during migration of a highly reactive superoxide anion across a solvent-exposed active site.[47,48]

Generation of the Y318F PHM variant made it possible to test whether reductive cleavage of a Cu_M(II)-hydroperoxo intermediate by a proximal and conserved active-site tyrosine could lead to formation of the reactive Cu_M(II)-oxo species (mechanism C).[54] A full kinetic analysis of the Y318F PHM mutant resulted in only a four-fold reduction in the rate for C−H bond cleavage, and the intrinsic hydrogen and ^{18}O isotope effects are nearly identical to that of WT PHM. Based on this comprehensive kinetic analysis, mechanism C was ruled out as well. A mechanism whereby the roles of the copper sites are reversed (mechanism E) is intriguing, but not supported by

experimental evidence. The compilation of kinetic, spectroscopic, and structural evidence supports a mechanism where substrate and O_2 activation take place at the Cu_M site.[27,32,33,35] The formation and utilization of a Cu_M(II)-peroxo (mechanism B) oxidizing intermediate is primarily based on the X-ray structure of PHM. The absence of any residues capable of general acid catalysis led to the proposal that a Cu_M(II)-peroxo species could be responsible for catalysis.[25,55] To test this hypothesis, reduced DβM was reacted with O_2 and an unreactive substrate analogue, β,β-difluorophenylethylamine.[50] Reduction of O_2 and the formation of a Cu_M(II)-peroxo intermediate is predicted to result in oxidation of both copper sites to Cu(II), which should be detectable by EPR. However, this study did not result in any observable Cu(II) EPR signal. Generation of a very low level of the Cu_M(II)-peroxo species, outside the sensitivity of the EPR experiments, could explain this result. However, the failure to observe any oxidized copper is best explained by the formation of a diamagnetic Cu_M(II)-superoxo intermediate (mechanism F), which is EPR silent.

The mechanism proposed by Klinman and co-workers[50] (Fig. 1.4) satisfies the extensive data available for DβM, PHM, and TβM. Substrate and O_2 bind to the reduced enzyme forming the ternary complex, which induces the initial O_2 activation involving ET from Cu_M(I)–dioxygen to form a Cu_M(II)–superoxo species.[50] The magnitude of ^{18}O KIEs using either protio- or deuterio-labeled substrates for DβM and PHM is consistent with this proposed mechanism (Table 1.1). For both enzymes, the magnitude of k_{16}/k_{18} increases with deuterated substrate, which reveals that the activation of substrate and O_2 must be coupled by a reversible chemical process.[38,43] The recently measured ^{18}O KIE for galactose oxidase, a mononuclear copper enzyme that undergoes hydrogen-atom transfer to a Cu(II)–superoxo species, is nearly identical to that determined for DβM/PHM.[56] The ^{18}O KIEs provide substantial evidence for a Cu_M(II)–superoxo species and establish a limiting KIE for hydrogen-atom abstraction by a Cu_M(II)–superoxo intermediate. Furthermore, density functional theory (DFT) calculations found the Cu_M(II)–superoxo species to be kinetically and thermodynamically more favorable than the Cu_M(II)–hydroperoxo intermediate.[57] Subsequently, the Cu_M(II)–superoxo intermediate abstracts a hydrogen atom from the substrate via a hydrogen tunneling mechanism.[38,42] A critical feature of this mechanism involves the timing and pathway for long-range transfer of the second electron from Cu_H(I). If ET from Cu_H(I) to Cu_M(II)–superoxo preceded C−H activation, it would have to happen significantly faster than C−H activation, which is estimated as $10^3\ s^{-1}$.[32,38] This scenario cannot be excluded in the event that the driving force (ΔG°) and reorganization energy (λ) are both relatively small.[58] However, the implication of Cu_M(II)–superoxo as the oxygen species responsible for C−H activation, together with the clear demonstration that C−H abstraction is irreversible,[40] requires that k_{cat}/K_m for O_2 and substrate be independent of the second ET from Cu_H.

The consensus mechanism places the long-range ET from Cu_H to Cu_M within k_{cat}.[59] The route of long-range ET has been proposed to involve substrate and/or a protein network.[49,59] When the Q170A PAM variant was generated to investigate the role of an interdomain, hydrogen-bonded protein network only minor effects on

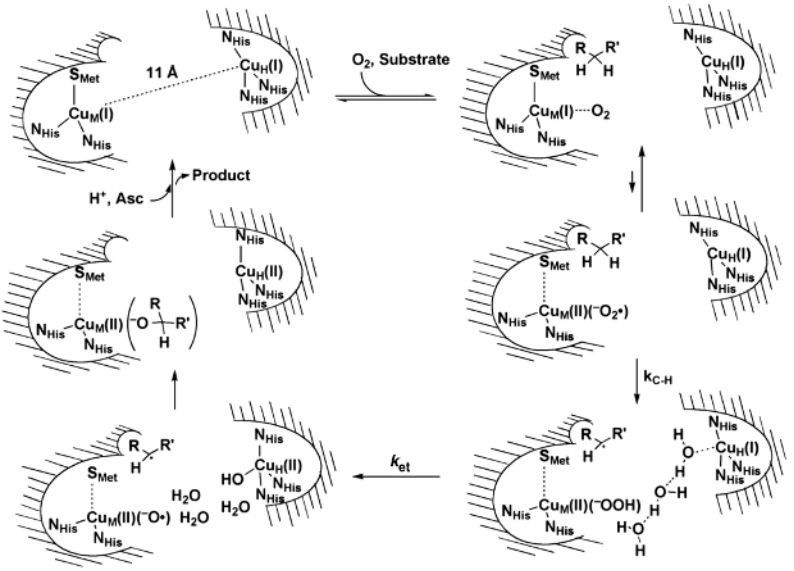

FIGURE 1.4. Copper-superoxo mechanism for DβM, PHM, and TβM. This research was originally published in the *Journal of Biological Chemistry*. Evans, J. P.; Ahn, K.; Klinman, J. P. Evidence that dioxygen and substrate activation are tightly coupled in dopamine β-monooxygenase. Implications for the reactive oxygen species[50] *J. Biol. Chem*. **2003**, *278*, 49691–49698. Copyright © The American Society for Biochemistry and Molecular Biology.

enzyme activity were observed, ruling out this pathway for ET from Cu_H to Cu_M.[49] Similarly, examination of the PHM-catalyzed reaction with two different substrates differing in length (Fig. 1.5) results in similar kinetic parameters (Table 1.2), indicating that the substrate backbone is an unlikely pathway for ET between copper sites.[59] The collective data on DβM and PHM are consistent with a mechanism in which long-range ET occurs within the solvent-exposed interface between Cu_M and Cu_H. As outlined in the proposed mechanism (Fig. 1.4), interdomain ET occurs after C−H activation, which reduces the transfer distance to $\sim$ 7 Å.[50] Water-mediated ET over this distance is thoroughly consistent with the experimentally measured values for k_{cat} for this class of enzymes ($\sim$ 3–40 s^{-1}).[32,38,39] Electron transfer from Cu_H to Cu_M is proposed to induce reductive cleavage of the Cu_M(II)–hydroperoxo intermediate yielding water and a Cu_M(II)–oxo radical, which recombines with the substrate radical to form an

1 **2**

FIGURE 1.5. The structures used in the study are from Ref. 59 and referred to in Table 1.2.

TABLE 1.2. Comparison of Kinetic Parameters for Truncated and Extended Peptide Substrates with PAM[a]

Substrate	$k_{cat}/K_m(O_2)$ (μM^{-1}, s^{-1})	$^D[k_{cat}/K_m(O_2)]$	k_{cat} (s^{-1})	$^Dk_{cat}$
1[b]	0.14 (0.01)	3.1 (0.3)	37 (0.1)	1.0 (0.1)
2[b]	0.23 (0.03)	2.3 (0.2)	17 (0.8)	1.0 (0.1)

[a] This table was derived from Ref. 59.
[b] Figure 1.5 illustrates the structure of the substrates used in this study denoted by "1" and "2" in the table.

inner-sphere alcohol product.[50] Alternatively, computational experiments suggest a thermodynamically favorable mechanism in which the substrate-derived radical abstracts a hydroxyl radical from the Cu_M(II)–hydroperoxo intermediate, and the resulting Cu_M(II)-oxo species is subsequently reduced via ET from Cu_H.[57] In reality, the net process is likely to be a concerted one, in which long-range ET occurs concomitant with the attack of substrate radical on the Cu_M(II)–hydroperoxo. However, the increase in k_{cat} for the oxidation of phenethylamine substrates with electron-withdrawing groups catalyzed by DβM has been interpreted to be the result of changes in the partially rate-limiting dissociation of the inner-sphere alcohol complex to form free product.[32] The intermediacy of an inner-sphere alcohol moiety is further supported by experimental evidence and QM/MM simulations for PAM catalysis with a non-natural substrate, benzaldehyde imino-oxy acetic acid.[60]

1.5. A NETWORK OF COMMUNICATION BETWEEN Cu_M AND Cu_H

How DβM, PHM, and TβM catalyze such tightly coupled reactions using two mononuclear Cu atoms separated by ~ 11 Å and completely exposed to solvent is still not well understood. In this section, evidence will be presented that supports the idea that subtle, but essential communication occurs between the mononuclear Cu sites and throughout the entire protein structure, which plays a central role in ensuring efficient wave function overlap between the hydrogen donor and the metal-superoxo species at the Cu_M site and in maintaining tight coupling between C−H and O_2 activation. A number of PHM variants have been generated, and the resulting data are generally analyzed in terms of how mutations near Cu_M and Cu_H impact the specific functions of each Cu site (i.e., C−H and O_2 activation and substrate hydroxylation at Cu_M and long-range ET at Cu_H). However, a trend is starting to emerge illustrating how an individual mutation at one copper domain impacts the other copper domain.

Kinetic analyses of the Y79F[4] and Y79W[49] PHM variants provided early evidence for a network of communication between the two copper domains, although the data were not initially discussed in this context. Based on sequence conservation and prior to any knowledge that Tyr79 of PHM is located ~ 4 Å from Cu_H, this residue was one of the first mutated within recombinant PHM.[4] The Y79F PHM variant has a significant impact on k_{cat}/K_m(substrate), giving a 15-fold decrease in rate (k_{cat})

TABLE 1.3. Relative Decrease in Kinetic Parameters for Variants of PHM Compared to WT PHM[a]

PHM/Mutants	k_{cat}	k_{cat}/K_m(S)	$k_{cat}/K_m(O_2)$	k_{C-H}
Y79F[b]	~ 15-fold	~ 60-fold		
Y79W[c]	~ 200-fold	~ 300-fold		
H172A[d]	~ 3000-fold		~ 300-fold	~ 12,000-fold

[a] The data in this table are given as relative decreases compared to WT PHM because exact values were not always provided for the kinetic parameters, and the substrates were not always the same from study to study. However, the same substrate was used when comparing the impact on kinetic parameters of each individual PHM variant to WT PHM.
[b] Data taken from Ref. 4.
[c] Data taken from Ref. 49.
[d] Data taken from Ref. 51.

relative to a WT PHM construct for the oxidation of α-*N*-acetyl-Tyr-Val-Gly (Table 1.3). Y79F PHM also exhibited an ~ four-fold increase in the K_m(substrate).[4] Based on this simple analysis, Y79F PHM results in an ~60-fold decrease for k_{cat}/K_m (substrate), which is the kinetic parameter that reports on C−H activation and substrate hydroxylation at the Cu_M site (Table 1.3). Y79W PHM was generated after a number of PHM crystal structures had been solved. The rationale for generating this variant was to use Trp79 as a fluorescent indicator that could be used to monitor the active site.[49] Additionally, a general kinetic examination of Y79W PHM was completed, and the largest effect observed (~ 300-fold reduction) was on the second-order rate constant, k_{cat}/K_m (substrate) (Table 1.3).[49] The impact of Y79F PHM on K_m (substrate) led to the suggestion that Tyr79 might interact with the glycyl moiety of glycine extended peptides[4]; little discussion was provided in regards to the impact of Y79F PHM on k_{cat}/K_m (substrate). The effect of Y79W PHM on the measured kinetic parameters in concert with the fluorescence measurements led to a proposed mechanism in which the roles of Cu_M and Cu_H are reversed.[49] Based on the current working mechanism (Fig. 1.4), we now propose that the two Tyr79 mutants disrupt a network of hydrogen-bonded water molecules connecting the separate copper domains. The Tyr79 residue may be critical for long-range ET based on the decrease in k_{cat}, but the largest impact for both variants is on the kinetic parameter k_{cat}/K_m (substrate), which measures C−H activation efficiency at Cu_M. The Tyr79 residue forms a pi–pi interaction with His172, a ligand to Cu_H, and replacement of this tyrosine with any amino acid likely invokes subtle changes in the coordination environment at Cu_H, which we now propose disrupts a network of connectivity that significantly impacts chemistry taking place at Cu_M.

A number of studies with Met314 PHM variants have been carried out to probe the importance of this residue during catalysis. Initial reports showed that substitution of Met314 with Ile, His, or Cys did not restore catalysis.[4,61] However, a recent study with TβM demonstrates that mutation of the parallel residue, Met471, to Cys retains activity while the Asp471 and His471 variants are inactive. Interestingly, M471C TβM undergoes a secondary inactivation pathway during turnover, and full conversion

of tyramine to octopamine is not observed under any conditions.[62] The coordination environment of the reduced Met471 variants was investigated by EXAFS, and slight, subtle differences for M471C TβM compared to the Asp471 and His471 mutants indicate the possibility of a small contribution from cysteine ligation.[29] This observation could account for the activity of M471C TβM. A crystallographic study with M314I PHM revealed a number of interesting results. Predictably, structural alignment between oxidized M314I PHM and the published structure of oxidized PHM showed significant changes close to the Cu_M site. Displacement of the mutated residue, Ile314, from Cu_M resulted in disorder of the flanking loop (299–313) and caused loop 212–218 to move as far as 5 Å away from Cu_M. Unexpectedly, replacement of the Met314 ligand does not prohibit copper binding at the Cu_M site. The Met314 residue is replaced with a water molecule, and the remaining coordinating ligands shift slightly to retain the distorted tetrahedral geometry. In fact, mutation of Met314 appears to have a more dramatic impact on the Cu_H domain, even though this domain resides 11 Å away from Cu_M. Specifically, His107 and Cu_H are highly disordered in the oxidized M314I PHM structure. At the same time, significant structural changes in the protein regions connecting the two copper domains were not observed.[63] These findings reinforce a previous EXAFS study, in which the occupancy of the Cu_H appears to be coupled to the movement of Met314 at Cu_M.[64] The significant impact on the coordination environment at Cu_H as a result of mutation of the methionine ligand to Cu_M further demonstrates the interconnectivity between the two domains and the sensitivity of each copper site to long-range perturbations.

Recently, an extensive kinetic and deuterium isotope study was completed for H172A PHM.[51] Histidine at position 172 is a ligand to the ET copper, Cu_H, and the H172A PHM variant retains copper binding and hydroxylase activity.[48] Changing the coordination environment at Cu_H was predicted to impact the long-range ET step without affecting other steps in the kinetic mechanism. Unexpectedly, both k_{cat} and $k_{cat}/K_m(O_2)$ for H172A PHM decrease significantly (Table 1.3), and the deuterium isotope effects on these parameters increase. For H172A PHM, C−H abstraction has become more rate-limiting, indicating that altering the coordination and the redox properties at Cu_H impacts the rate of chemistry taking place at Cu_M.[51] The impact of mutating His172 was further examined by determining the intrinsic rate constants (Scheme 1.1), which can be calculated from the measured kinetic parameters, their isotope effects, and the intrinsic isotope effect. The intrinsic isotope effect for H172A PHM was not determined, but the value was determined previously for WT PHM[38] and assumed to be similar for H172A PHM. Remarkably, this approach leads to an estimated ∼12,000-fold decrease in the rate of the hydrogen-transfer step for H172A PHM (Table 1.3). Now we propose that the dramatic impact on the rate of C−H cleavage is due to subtle, but critical, changes to a water-mediated hydrogen-bonding network linking the two mononuclear copper domains.

Re-examination of the existing family of PHM crystal structures shows a conserved network of waters from His108, bound to Cu_H, to the peptide backbone carbonyl of His244 or Met314, a ligand to Cu_M (Fig. 1.6). This network is present in all of the structures, and does not appear to be dependent on the presence of substrate or the oxidation state of the coppers. Herein, we suggest that this network could be one of the

primary structural features that links the two copper domains. The observation that substitution of His108 with alanine eliminated detectable activity for PHM, and the fact that this residue is the only Cu_H ligand observed to move when comparing the oxidized and reduced structures is consistent with our hypothesis.[4,63] If this network couples the two copper sites, substitution of any active-site residue at Cu_H might disrupt substrate binding at Cu_M such that its orientation becomes nonoptimal for C−H cleavage. As discussed above, the transfer of hydrogen from substrate to the activated oxygen species in WT PHM transpires via hydrogen tunneling.[38,42] We believe the PHM data can be fully understood in the context of a model for hydrogen tunneling in enzyme-catalyzed reactions that requires the contribution of two types of protein motions to achieve effective wave function overlap between the hydrogen

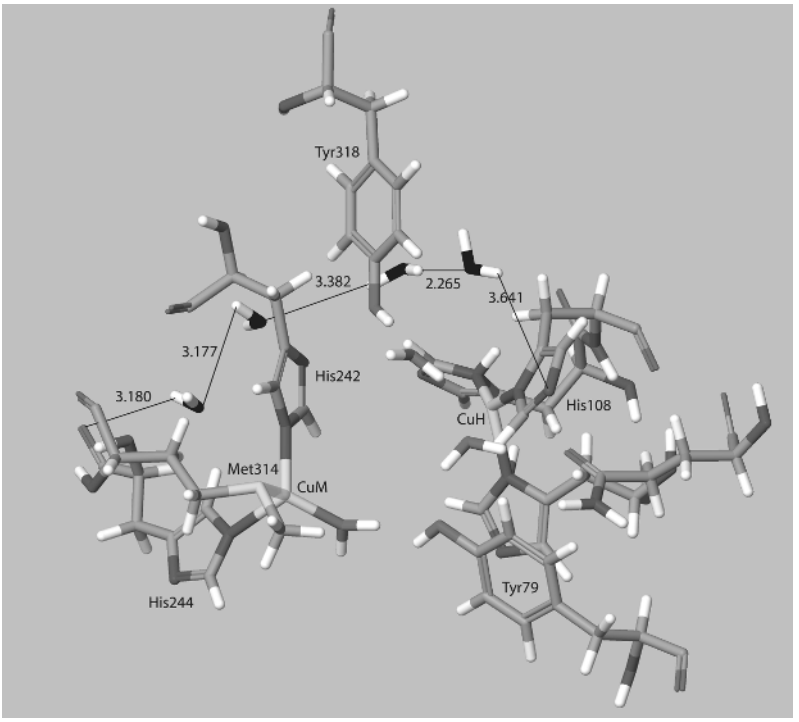

FIGURE 1.6. Active-site structure of reduced PHM recreated from PDB: 3PHM.[55] The copper atoms (Cu_M to the left and Cu_H to the right), coordinating ligands, Tyr79 (bottom), and Tyr318 (top) are colored by atom type (carbon is gray, nitrogen is blue, sulfur is yellow, oxygen is red, copper is aqua, and hydrogen is white). The proposed network of connectivity between Cu_H and Cu_M through hydrogen-bonded water molecules is shown (oxygen atoms of networked waters are shown in black for clarity). Other active-site water molecules that might stabilize the active site and/or contribute to a pathway of long-range ET are shown (oxygen atoms of water molecules are red). The active-site structure was recreated using the program Maestro. (See color insert.)

donor and acceptor.[65] The first type of motion has been labeled preorganization and reflects the sampling of a large number of protein conformational substates, with only a small subset of conformers optimized for tunneling to occur in the WT enzyme. Once the family of preorganized conformations has been achieved, reorganization invokes heavy atom motions to achieve barrier crossing. Disturbing the network of connectivity by making mutations at Cu_H could have a significant impact on the ability of the enzyme to find catalytically relevant conformers resulting in dramatic impacts on the rate of C−H activation taking place at Cu_M. A structured solvent-exposed active site, comprised of ordered water molecules, is likely a required feature for this small family of enzymes orchestrating the intricate and tightly coupled chemistry that transpires.

1.6. CONCLUDING REMARKS AND FUTURE PROSPECTS

Herein, we present a review of the literature relating to the mechanism for reactions catalyzed by DβM, PHM, and TβM. Specifically, experimental evidence for the structure of the activated oxygen intermediate, the nature of hydrogen transfer, and how C−H and O_2 activation are coupled have been discussed. Based on the multiple X-ray structures available for PHM, we propose a network of connectivity between the two mononuclear copper domains (Fig. 1.6). Researchers have spent an abundant amount of energy trying to explain the anomalous nature of the solvent-exposed active site that is characteristic of this small class of enzymes. We suggest that nature has engineered these enzymes to utilize water as a specific medium for communication between the separate active-site domains from Cu_H to Cu_M in a way that may prevent deleterious uncoupling reactions. For the future, appropriately designed experiments and computations are needed to clarify the precise pathway of long-range ET and to provide more insight into the nature of backbone connectivity between the fully solvent-exposed copper domains that characterize this unique family of enzymes.

ABBREVIATIONS

Asc	Ascorbate
Asp	Aspartate
Cys	Cysteine
DβM	Dopamine β-monooxygenase
DFT	Density functional theory
EPR	Electron paramagnetic resonance
ET	Electron transfer
EXAFS	Extended X-ray absorption fine structure
His	Histidine
Ile	Isoleucine
KIE(s)	Kinetic isotope effect(s)

Met	Methionine
PAM	Peptidylglycine α-amidating monooxygenase
PHM	Peptidylglycine α-hydroxylating monooxygenase
QM/MM	Quantum mechanical/molecular mechanics
TβM	Tyramine β-monooxygenase
Tyr	Tyrosine
WT	Wild type
XAS	X-ray absorption spectroscopy

REFERENCES

1. Malmstrom, B. G. Enzymology of oxygen *Ann. Rev. Biochem.* **1982**, *51*, 21–59.
2. Klinman, J. P. Mechanisms whereby mononuclear copper proteins functionalize organic substrates *Chem. Rev.* **1996**, *96*, 2541–2561.
3. Klinman, J. P. The copper-enzyme family of dopamine β-monooxygenase and peptidylglycine α-hydroxylating monooxygenase: Resolving the chemical pathway for substrate hydroxylation *J. Biol. Chem.* **2006**, *281*, 3013–3016.
4. Eipper, B. A.; Quon, A. S. W.; Mains, R. E.; Boswell, J. S.; Blackburn, N. J. The catalytic core of peptidylglycine α-hydroxylating monooxygenase: Investigation by site-directed mutagenesis, Cu X-ray absorption spectroscopy, and electron paramagnetic resonance *Biochemistry* **1995**, *34*, 2857–2865.
5. Orchard, I.; Ramirez, J.; Lange, A. B. A multifunctional role for octopamine in locus flight *Ann. Rev. Entomol.* **1993**, *38*, 227–249.
6. Kim, C-H.; Zabetian, C. P.; Cubells, J. F.; Cho, S.; Biaggioni, I.; Cohen, B. M.; Robertson, D.; Kim, K-S. Familial paraganglioma and gastric stromal sarcoma: A new syndrome distinct from the Carney triad *Am J. Med. Genet.* **2002**, *108*, 140–147.
7. Timmers, H. J. L. M.; Deinum, J.; Wevers, R. A.; Lenders, J. W. M. Congenital dopamine-β-hydroxylase deficiency in humans *Ann. N. Y. Acad. Sci.* **2004**, *1018*, 520–523.
8. Cubells, J. F.; Zabetian, C. P. Human genetics of plasma dopamine β-hydroxylase activity: Applications to research in psychiatry and neurology *Psychopharmacology* **2004**, *174*, 463–476.
9. Prigge, S. T.; Mains, R. E.; Eipper, B. A.; Amzel, L. M. New insights into copper monooxygenases and peptide amidation: Structure, mechanism and function *Cell Mol. Life Sci.* **2000**, *57*, 1236–1259.
10. Roeder, T. Tyramine and octopamine: Ruling behavior and metabolism *Annu. Rev. Entomol.* **2005**, *50*, 447–477.
11. Lehman, H. K.; Schulz, D. J.; Barron, A. B.; Wraight, L.; Hardison, C.; Whitney, S.; Takeuchi, H.; Paul, R. K.; Robinson, G. E. Division of labor in the honey bee (*Apis mellifera*): The role of tyramine β-hydroxylase *J. Exp. Biol.* **2006**, *209*, 2774–2784.
12. Monastirioti, M. Distinct octopamine cell population residing in the CNS abdominal ganglion controls ovulation in *Drosophila melanogaster Dev. Biol.* **2003**, *264*, 38–49.
13. Winkler, H.; Carmichael, S. W. *The Secretory Granule*, A. M. Poisner and J. M. Trifaro, Eds., Elsevier Biomedical Press, Amsterdam, The Netherlands, **1982**.

14. Stewart, L. C.; Klinman, J. P. Dopamine beta-hydroxylase of adrenal chromaffin granules: Structure and function *Annu. Rev. Biochem.* **1988**, *57*, 551–592.
15. Eipper, B. A.; Stoffers, P. A.; Mains, R. E. The biosynthesis of neuropeptides: Peptide α-amidation *Annu. Rev. Neurosci.* **1992**, *15*, 57–85.
16. Klinman, J. P.; Krueger, M.; Brenner, M.; Edmondson, D. E. Evidence for two copper atoms/subunit in dopamine beta-monooxygenase catalysis *J. Biol. Chem.* **1984**, *259*, 3399–3402.
17. Skotland, T.; Ljones, T. Direct spectrophotometric detection of ascorbate free radical formed by dopamine β-monooxygenase and by ascorbate oxidase *Biochim. Biophys. Acta* **1980**, *630*, 30–35.
18. Diliberto, E. J., Jr.; Allen, P. L. Mechanism of dopamine-β-hydroxylation. Semidehydroascorbate as the enzymic oxidation product of ascorbate *J. Biol. Chem.* **1981**, *256*, 3385–3393.
19. Brenner, M. C.; Klinman, J.P. Correlation of copper valency with product formation in single turnovers of dopamine beta-monooxygenase *Biochemistry* **1989**, *28*, 4664–4670.
20. Freeman, J. C.; Villafranca, J. J.; Merkler, D. J. Redox cycling of enzyme-bound copper during peptide amidation *J. Am. Chem. Soc.* **1993**, *115*, 4923–4924.
21. Gray, E. E.; Small, S. N.; McGuirl, M. A. Expression and characterization of recombinant tyramine β-monooxygenase from *Drosophila*: A monomeric copper-containing hydroxylase *Prot. Exp. Purif.* **2006**, *47*, 162–170.
22. Lamouroux, A.; Vigny, A.; Faucon Biguet, V.; Darmon, M. C.; Frank, R.; Henry, J. P.; Mallet, J. The primary structure of human dopamine-beta-hydroxylase: Insights into the relationship between the soluble and the membrane-bound forms of the enzyme *EMBO J.* **1987**, *6*, 3931–3937.
23. Southan, C.; Kruse, L. I. Sequence similarity between dopamine β-hydroxylase and peptide α-amidating enzyme: Evidence for a conserved catalytic domain *FEBS Lett*. **1989**, *255*, 116–120.
24. Chenna, R.; Sugawara, H.; Koike, T.; Lopez, R.; Gibson, T. J.; Higgins, D. G.; Thompson, J. D. Multiple sequence alignment with the Clustal series of programs *Nucleic Acids Res.* **2003**, *31*, 3497–3500.
25. Prigge, S. T.; Eipper, B. A.; Mains, R. E.; Amzel, L. M. Amidation of bioactive peptides: The structure of peptidylglycine α-hydroxylating monooxygenase *Science* **1997**, *278*, 1300–1305.
26. Boswell, J. S.; Reedy, B. J.; Kulathila, R.; Merkler, D.; Blackburn, N. J. Structural investigations on the coordination environment of the active-site copper centers of recombinant bifunctional peptidylglycine α-amidating enzyme *Biochemistry* **1996**, *35*, 12241–12250.
27. Reedy, B. J.; Blackburn, N. J. Preparation and characterization of half-apo dopamine-β-hydroxylase by selective removal of CuA. Identification of a sulfur ligand at the dioxygen binding site by EXAFS and FTIR spectroscopy *J. Am. Chem. Soc.* **1994**, *116*, 1924–1931.
28. Scott, R. A.; Sullivan, R. J.; DeWolf, W. E.; Dolle, R. E.; Kruse, L. I. The copper sites of dopamine β-hydroxylase: An x-ray absorption spectroscopic study *Biochemistry* **1988**, *27*, 5411–5417.

29. Hess, C. R.; Klinman, J. P.; Blackburn, N. J. The copper centers of tyramine β-monooxygenase and its catalytic-site methionine variants. An x-ray absorption study. *J. Biol. Inorg. Chem.* **2010**, *15*, 1195–1207.
30. Fitzpatrick, P. F.; Villafranca, J. J. Mechanism-based inhibitors of dopamine beta-hydroxylase containing acetylenic or cyclopropyl groups *J. Am. Chem. Soc.* **1985**, *107*, 5022–5023.
31. Fitzpatrick, P. F.; Flory, D. R., Jr.; Villafranca, J. J. 3-Phenylpropenes as mechanism-based inhibitors of dopamine beta-hydroxylase: Evidence for a radical mechanism *Biochemistry* **1985**, *24*, 2108–2114.
32. Miller, S. M.; Klinman, J. P. Secondary isotope effects and structure–reactivity correlations in the dopamine beta-monooxygenase reaction: Evidence for a chemical mechanism *Biochemistry* **1985**, *24*, 2114–2127.
33. Blackburn, N. J.; Pettingill, T. M.; Seagraves, K. S.; Shigeta, R. T. Characterization of a carbon monoxide complex of reduced dopamine β-hydroxylase. Evidence for inequivalence of the Cu(I) centers *J. Biol. Chem.* **1990**, *265*, 15383–15386.
34. Cook, P. F.; Cleland, W. W. Mechanistic deductions from isotope effects in multireactant enzyme mechanisms *Biochemistry* **1981**, *20*, 1790–1796.
35. Prigge, S. T.; Eipper, B. A.; Mains, R. E.; Amzel, L. M. Dioxygen binds end-on to mononuclear copper in a precatalytic complex *Science* **2004**, *304*, 864–867.
36. Klinman, J. P.; Humphries, H.; Voet, J. G. Deduction of kinetic mechanism in Multisubstrate enzyme reactions from tritium isotope effects *J. Biol. Chem.* **1980**, *255*, 11648–11651.
37. Friedman, S.; Kaufman, S. 3,4-Dihydroxyphenylethylamine beta-hydroxylase. Physical properties, copper content, and role of copper in the catalytic activity. *J. Biol. Chem.* **1965**, *240*, 4763–4773.
38. Francisco, W. A.; Merkler, D. J.; Blackburn, N. J.; Klinman, J. P. Kinetic mechanism and intrinsic isotope effects for the peptidylglycine α-amidating enzyme reaction *Biochemistry* **1998**, *37*, 8244–8252.
39. Hess, C. R.; McGuirl, M. M.; Klinman, J. P. Mechanism of the insect enzyme, tyramine β-monooxygenase, reveals differences from the mammalian enzyme, dopamine β-monooxygenase *J. Biol. Chem.* **2008**, *283*, 3042–3049.
40. Miller, S. M.; Klinman, J. P. Magnitude of intrinsic isotope effects in the dopamine β-monooxygenase reaction *Biochemistry* **1983**, *22*, 3091–3096.
41. Northrop, D. B. Steady state analysis of kinetic isotope effects in enzymatic reactions *Biochemistry* **1975**, *14*, 2644–2651.
42. Francisco, W. A.; Knapp, M. J.; Blackburn, N. J.; Klinman, J. P. Hydrogen tunneling in peptidylglycine α-hydroxylating monooxygenase *J. Am. Chem. Soc.* **2002**, *124*, 8194–8195.
43. Tian, G.; Berry, J. A.; Klinman, J. P. Oxygen-18 kinetic isotope effects in the dopamine β-monooxygenase reaction: Evidence for a new chemical mechanism in non-heme metallomonooxygenases *Biochemistry*, **1994**, *33*, 226–234.
44. Schneider, M. E.; Stern, M. J. Arrhenius preexponential factors for primary hydrogen kinetic isotope effects *J. Am. Chem. Soc.* **1972**, *94*, 1517–1522.
45. Bell, R. P. *The Tunnel Effect in Chemistry*; Chapman & Hall: New York, 1980.
46. Melander, L.; Saunders, W. H. J. *Reaction Rates of Isotopic Molecules*; John Wiley & Sons, Inc.: New York, 1980.

47. Jaron, S.; Blackburn, N. J. Does superoxide channel between the copper centers in peptidylglycine monooxygenase? A new mechanism based on carbon monoxide reactivity *Biochemistry* **1999**, *38*, 15086–15096.
48. Jaron, S.; Mains, R. E.; Eipper, B. A.; Blackburn, N. J. The catalytic role of the copper ligand H172 of peptidylglycine alpha-hydroxylating monooxygenase (PHM): A spectroscopic study of the H172A mutant *Biochemistry* **2002**, *41*, 13274–13282.
49. Bell, J.; El Meskini, R.; D'Amato, D.; Mains, R. E.; Eipper, B. A. Mechanistic investigation of peptidylglycine α-hydroxylating monooxygenase via intrinsic tryptophan fluorescence and mutagenesis *Biochemistry* **2003**, *42*, 7133–7142.
50. Evans, J. P.; Ahn, K.; Klinman, J. P. Evidence that dioxygen and substrate activation are tightly coupled in dopamine beta-monooxygenase. Implications for the reactive oxygen species *J. Biol. Chem.* **2003**, *278*, 49691–49698.
51. Evans, J. P.; Blackburn, N. J.; Klinman, J. P. The catalytic role of the copper ligand H172 of peptidylglycine α-hydroxylating monooxygenase: A kinetic study of the H172A mutant *Biochemistry*, **2006**, *45*, 15419–15429.
52. Solomon, E. I.; Brunold, T. C.; Davis, M. I.; Kemsley, J. N.; Lee, S. –K.; Lehnert, N.; Neese, R.; Skulan, A. J.; Yang, Y. –S.; Zhou, J. Geometric and electronic structure/function correlations in non-heme iron enzymes *Chem. Rev.* **2000**, *100*, 235–349.
53. Gorsky, L. D.; Koop, D. R.; Coon, M. J. On the stoichiometry of the oxidase and monooxygenase reactions catalyzed by liver microsomal cytochrome P-450. Products of oxygen reduction *J. Biol. Chem.* **1984**, *259*, 6812–6817.
54. Francisco, W. A.; Blackburn, N. J.; Klinman, J. P. Oxygen and hydrogen isotope effects in an active site tyrosine to phenylalanine mutant of peptidylglycine α-hydroxylating monooxygenase: Mechanistic implications *Biochemistry* **2003**, *42*, 1813–1819.
55. Prigge, S. T.; Kolhekar, A. S.; Eipper, B. A.; Mains, R. E.; Amzel, L. M. Substrate-mediated electron transfer in peptidylglycine α-hydroxylating monooxygenase *Nature (London)* **1999**, *6*, 976–983.
56. Humphreys, K. J.; Mirica, L. M.; Wang, Y.; Klinman, J. P. Galactose oxidase as a model for reactivity at a copper superoxide center *J. Am. Chem. Soc.* **2009**, *131*, 4657–4663.
57. Chen, P.; Solomon, E. I. Oxygen activation by the noncoupled binuclear copper site in peptidylglycine alpha-hydroxylating monooxygenase. Reaction mechanism and role of the noncoupled nature of the active site *J. Am. Chem. Soc.* **2004**, *126*, 4991–5000.
58. Personal communication with Harry B. Gray.
59. Francisco, W. A.; Wille, G.; Smith, A. J.; Merkler, D. J.; Klinman, J. P. Investigation of the pathway for inter-copper electron transfer in peptidylglycine α-amidating monooxygenase *J. Am. Chem. Soc.* **2004**, *126*, 13168–13169.
60. McIntyre, N. R.; Lowe, Jr., E. W.; Merkler, D. J. Imino-oxy acetic acid dealkylation as evidence for an inner-sphere alcohol intermediate in the reaction catalyzed by peptidylglycine α-hydroxylating monooxygenase *J. Am. Chem. Soc.* **2009**, *131*, 10308–10319.
61. Kolhekar, A. S.; Keutmann, H. T.; Mains, R. E.; Quon, A. S.; Eipper, B. A. Peptidylglycine alpha-hydroxylating monooxygenase: active site residues, disulfide linkages, and a two domain model of the catalytic core *Biochemistry* **1997**, *36*, 10901–10909.
62. Hess, C. R.; Wu, Z.; Ng, A.; Gray, E. E.; McGuirl, M. M.; Klinman, J. P. Hydroxylase activity of Met471Cys tyramine β-monooxygenase *J. Am. Chem. Soc.* **2008**, *130*, 11939–11944.

63. Siebert, X.; Eipper, B. A.; Mains, R. E.; Prigge, S. T.; Blackburn, N. J.; Amzel, L. M. The catalytic copper of peptidylglycine α-hydroxylating monooxygenase also plays a critical structural role *Biophys. J.* **2005**, *89*, 3312–3319.
64. Jaron, S.; Blackburn, N. J. Characterization of the half-apo derivative of peptidylglycine monooxygenase. Insight into the reactivity of each active site copper *Biochemistry* **2001**, *40*, 6867–6875.
65. Nagel, Z. D.; Klinman, J. P. Tunneling and dynamics in enzymatic hydride transfer *Chem. Rev.* **2006**, *106*, 3095–3118.